Available online at www.sciencedirect.com

ScienceDirect

Procedia Engineering 64 (2013) 720 – 726

Procedia Engineering

www.elsevier.com/locate/procedia

International Conference On DESIGN AND MANUFACTURING, IConDM 2013

Wear, Hardness and Corrosion Resistance Characteristics of Tungsten Sulfide Incorporated Electroless Ni-P Coatings

S.Karthikeyan[a]*, P.A.Jeeva[b], N.Arivazhagan[b], V. Umasankar[b], K.N.Srinivasan[c], M. Paramasivam[c]

[a]*Surface Engineering Research Laboratory, Centre for Nanobiotechnology, VIT University, Vellore- 632014, India*
[b] *School of Mechanical and Building Sciences, VIT University, Vellore-632014, India.*
[c] *CSIR-Central Electrochemical Research Institute,Karaikudi-630006, India*

Abstract

A novel composite coating containing WS_2 in Ni-P matrix was obtained by electroless deposition route. The incorporation of tungsten sulfide particles enhanced the hardness and corrosion resistance of the Ni-P coatings. It was established that the electroless Ni-P-WS_2 coatings were able to sustain the low coefficients of friction under severe sliding condition in comparison with the Ni-P coatings. It is evident that the Ni-P-WS_2 coatings have the option of being used as solid lubricants to the sliding parts of machineries in aerospace industries. The incorporation of WS_2 and the existence of Ni_3P in the matrix have been ascertained by XRD, SEM and AFM.

Keywords: wear, composites, lubricants, hardness, corrosion

Nomenclature

Nomenclature	
R_a	average roughness (nm)
Rq	root mean square roughness (nm)
R_{PV}	mean of maximum peak-to-valley height (nm)
R_t	charge transfer resistance (Ohm cm^2)
C_{dl}	double layer capacitance ($\mu F\ cm^{-2}$)
XRD	X-ray diffraction
SEM	scanning electron microscope
AFM	atomic force microscopy
XRF	X-ray fluorescence

1. Introduction

The ultra light metal of aluminium and its alloys are widely applied to the fields of aerospace, automobile, electronic products, etc. However, the surface of aluminium and its alloys needs to be protected due to the poor wear and corrosion resistance. Electroless composite coatings including Ni–P–Al_2O_3[1], Ni–P–MoS_2[2-3], Ni–P–PTFE [4-6], Ni–P–SiC [7-9], Ni-P-Graphite [10] and few other coatings [11-13] are synthesized by adding ceramic powders into the plating solution as a suspension during the plating process, so that the powders can be incorporated into the coating matrix . Aluminium alloys are “difficult to plate metal” based on the following reasons (1) The formation of passive oxide layer on the surface of aluminium alloys to deteriorate the coatings adhesion; (2) the in homogenous microstructure consisting of the primary phase and the second phase will result in the uneven coatings; Thus, electroless plating on aluminium alloys meets serious challenge. In order to satisfy the requirements for sliding parts with both low friction , good wear and corrosion resistance under dry condition mainly for aerospace industries, composite coatings incorporating some transition

* Corresponding author. Tel.:+91 78453 00117; fax: +91-416-2243092
E-mail address: skarthikeyanphd@yahoo.co.in; karthikeyan.s@vit.ac.in

Selection and peer-review under responsibility of the organizing and review committee of IConDM 2013
doi:10.1016/j.proeng.2013.09.147

metal dichalcogenides (disulfides) like MoS_2 , WS_2 etc., with low friction must be developed. Among them, tungsten disulphide posses good lubrication and corrosion resistance properties. Owing to strong hydrophobic character of WS_2, its incorporation is found complexity in electroless plating process. In this paper, electroless composite plating Ni–P–WS_2 process was developed. Then, the mechanical properties of the multilayer coatings consisting of electroless Ni–P–WS_2 and Ni–P coatings were investigated.

2. Experimental procedure

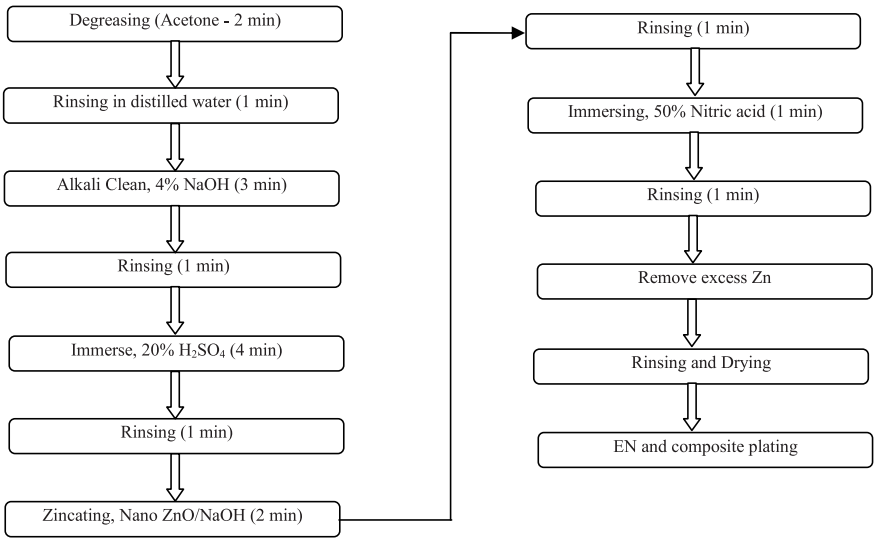

Fig. 1. Sequences of process for electroless Ni-P-WS_2 coatings.

Pure aluminium samples (99.9%) of size (10 cm × 10 cm × 0.3 cm) were used as the substrates. Specimens were mechanically polished using a SiC paper to a grit of 1000, then degreased ultrasonically in acetone. The process carried out for obtaining electroless composite plating Ni–P–WS_2 is given in figure 1. The compositions and operation conditions of electroless plating Ni–P were as follows: basic nickels carbonate 15 $g.l^{-1}$, sodium hypophosphite 28 $g.l^{-1}$, sodium citrate 30 $g.l^{-1}$, ammonium fluoride 11 $g.l^{-1}$, Thallium nitrate 0.02 $g.l^{-1,}$ pH 5.8, temperature 87 ◦C. To the above electroless plating solution, 2-20 $g.l^{-1}$ of WS_2 (size- 2µm) were added to the electroless composite plating solution. Before addition, the composite particle is blended with small amount of wetting agent (0.1 $g.l^{-1}$) as propitiatory sludge. The bath was agitated by mechanical stirrer with 310 rpm. The thickness of deposit was 12 μmh^{-1} measured using XRF spectroscopy (AMI, USA) and the plating duration was 5 hours.

The determination of phosphorus in the deposits of Ni-P is based on completely precipitating phosphorus as ammonium phosphomolybdate, dissolving the precipitate in 1N HNO_3 and excess HNO_3 was estimated by back titration. Nickel was analyzed by complexometric titration using EDTA with murexide as indicator. WS_2 particle content in composite coatings was calculated by the equation: C = (weight of WS_2 / Coating weight) × 100. Ni- P deposits dissolved in the solution of HNO_3 completely. WS_2 particles do not react with HNO_3, which was precipitated in the solution. The entire solution was placed for one week in order to completely precipitate WS_2 particles. Then the WS_2 particles were separated and dried at 95 °C for 16 h. Finally, the dried particles WS_2 were weighed on an electronic balance with an accuracy of 0.01 mg. The Vickers hardness coated composites as plated and annealed condition 400°C were evaluated at a load 100 g with a diamond pyramid indenter technique where time of indentation was 15 s. The results were an average of 5 times measurements.

Taber abrasion resistance with CS-10 abrasive wheel having a load of 1 kg for 1000 cycles was performed on Ni-P and Ni-P- WS_2 coatings. For the studies of corrosion, EG & G Princeton Applied Research Model 6310 was used. To that extent one cm^2 electrolessly deposited Ni-P and Ni-P- WS_2 were used as working electrodes. 4 cm^2 of platinum and saturated calomel electrodes were used as auxiliary and reference electrodes. The electrolyte was 3.5% NaCl. SEM and XRD (model ES 1640 A) measurements were conducted for determining the surface morphology and phase transition of coatings. Friction tests were conducted using a pin-on-disc tribometer. The block diagram of pin-on-disc apparatus is given in figure 2. The samples were cut into 10×10 mm squares and mounted on a stationary holder. The size of hole to hold the pin was 5 mm and the thickness of sample was 10 mm. A constant load of 3 N was impulsed on specimen under press along with 220 grit silicon carbide wear paper. The operating velocity of disc rotation was five rotations per minute and speed was 15.7 mm per second. The duration of pin-on-disc experiment was ten minutes.

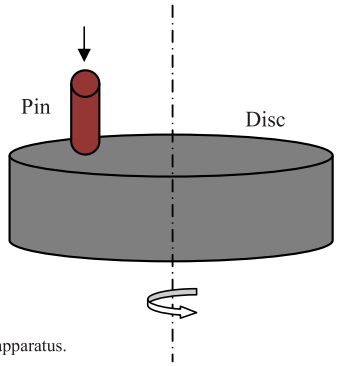

Specifications
1. Hardened Steel Disc, diameter = 20 cm^2, Speed = 2700 rpm
2. Pins(Al, Brass), diameter = 12 mm

Fig. 2. Block diagram for pin on disc apparatus.

3. Results and discussion

3.1 Structure

Figure 3 shows diffractograms of electroless composite coatings, after heat treatment at 400 ^oC. Nickel phosphide (Ni_3P) phase precipitates in the matrix and diffractograms show discrete peaks corresponding to crystalline Ni_3P and embedded WS_2 particles. The annealing process originates deposit grains to undergo significant growth, comprised good number of WS_2 in Ni-P matrix.

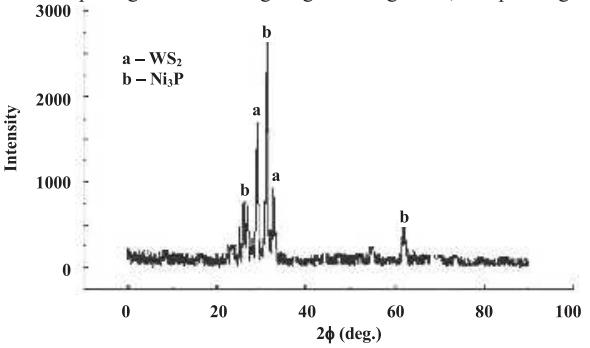

Fig. 3. X-ray diffraction patterns of the annealed EN - WS_2

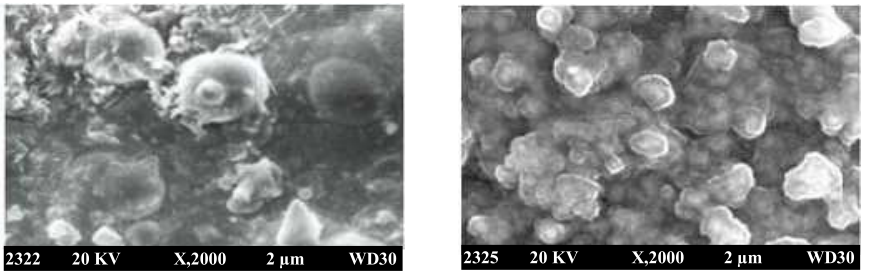

(a) (b)

Fig. 4. SEM images of (a) Ni–P (b) Ni–P - WS_2 coatings.

SEM images show the surface morphologies of the conventional Ni–P coating and Ni–P– WS_2 composite coatings. The coatings exhibited typical spherical nodular and layered structures of Ni-P deposits (Figure 4a). The agglomeration and crowding of WS_2 particles is visibly seen in Ni-P matrix (Figure 4b).

3.2. Cross sectional profile of composite coatings

AFM image analysis was carried out on composite coatings as well as with polished aluminium surface to understand average value of roughness R_a and root mean square roughness R_q.

Table 1 AFM data for composite coatings

Samples	Root mean square roughness, R_q	Average roughness, R_a	Mean of maximum Peak-to-Valley Height
Polished Aluminium	0.022 (µm)	0.017 (µm)	0.075(µm)
EN-P coatings	132.14(nm)	118.23(nm)	420.7(nm)
EN-P-WS_2 coatings	46.93 (nm)	40.45 (nm)	157.39 (nm)

Rq is much more sensitive than Ra to large and small height deviations from the mean. Table 1 is a summary of the Rq, Ra, R_{PV} values of polished aluminium, electroless Ni-P and composite coatings.

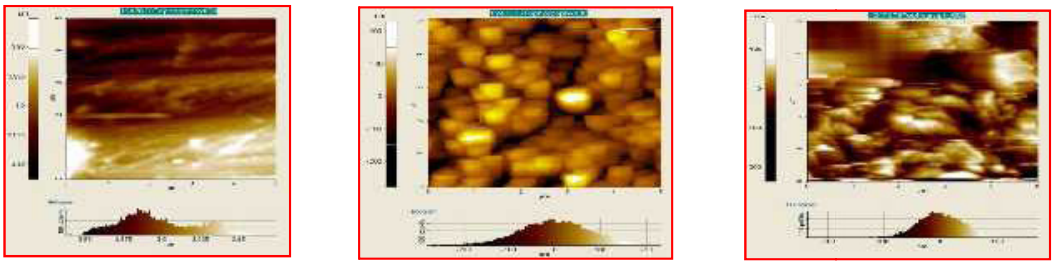

(a) (b) (c)

Fig. 5. Cross sectional AFM images of (a) polished Al; (b) Ni–P; (c) Ni–P - WS_2 coatings.

The value of Rq, Ra, R_{PV} height for the polished metal surface [reference sample] are 0.022 nm, 0.017nm, and 0.075 nm respectively, The slight roughness observed on the polished aluminium (Figure 5a) metal surface is due to atmospheric corrosion. The Rq, Ra, and R_{PV} height values for EN-P coatings (Figure 5b) are 132.14 nm, 118.23 nm, and 420.700 nm respectively. These data suggests the EN-P has a greater surface roughness than the polished metal surface. The presence of WS_2 reduces the Rq to 46.93 nm from 132.19 nm, and the average roughness is significantly reducing 40.45 nm when compared with 118.23 nm of EN-P. The maximum peak-to-valley height also was reduced to 157.39 nm. These parameters confirm that the surface appears smoother. The smoothness of the surface is due to the formation of soft WS_2 layers (Figure 5c) on the metal surface there by reduces the corrosion.

3.3. Hardness and wear resistance measurements

Table 2 summarizes Vickers micro hardness and wear tests, of Ni-P and Ni-P-WS_2 composite coatings as-deposited and after heat treatment at 400 °C for 4 hours. The hardness values of Ni-P coatings as plated and heat-treated are analogous to those obtained for Ni-P-SiC and Ni-P-Al_2O_3 coatings with a similar phosphorous content [14-15]. The enhanced hardness in the case of the composite (15 $g.l^{-1}$ of WS_2) after annealing at 400°C for 4 h is attributed to the precipitation of intermetallic phases induced by WS_2 particles incorporated aluminium in 3.5% NaCl. It has been noted that both hardness as well as abrasion resistance were found to increase as the bath loadings from 5 to 15 $g.l^{-1}$ of WS_2. Beyond 15 $g.l^{-1}$ a declined trend in the above mechanical properties is visibly noticed. This could be due to the collisions among the composite particles that may impede the deposition of Ni-P with subsequent entrapment of WS_2. Hence the optimum concentration for obtaining good results of hardness and abrasion resistance is fixed as 15 $g.l^{-1}$ of WS_2.

The improvement in the hardness of composite coatings might be due to the dispersion hardening effect caused by WS_2 particles in the composite matrix, which hinders the shift of displacement in nickel matrix. The higher hardness value of coatings containing Ni- 9.04% P – 6.28% WS_2 can be ascribed to both the hard particles and Ni_3P loaded matrix. The wear resistance Ni- 9.04% P – 6.28% WS_2 is found to be higher than the Ni-10.82% P - 0% WS_2 demonstrating that the improved results are due to WS_2 content. The wear resistance of both deposits is greatly enhanced after the heat treatment procedure.

Table 2. Effect of concentration of WS_2 particles in the bath on the hardness and wear resistance of the coating

Concentration of WS_2 in the bath g l^{-1}	Vicker's Hardness (load 100 g)		Weight loss (mg)	
	As plated	Annealed (400°C)	As plated	Annealed (400 °C)
0	490	610	7.9	5.0
5	629	749	6.0	3.1
10	810	965	5.1	1.4
15	1010	2114	1.2	0.09
25	980	1100	4.2	3.3

Figure 6 shows the relationship between the coefficients of friction and sliding time of Ni-P and Ni-P-WS_2 coatings. The coefficient of friction of the Ni-P coatings was 0.19 with increasing sliding timings up to 600 seconds. For Ni-P- WS_2 coatings, the coefficient of friction values was 0.14 up to a sliding distance of 600 seconds. It showed that the composite films had not been worn out in the tests. Ni-P-WS_2 composite coatings efficiently reduced the frictional coefficient of aluminium.

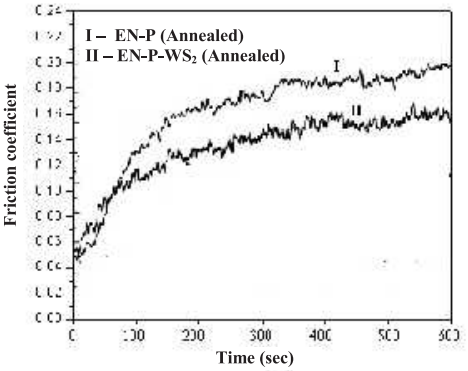

Fig. 6. Frictional coefficient Vs sliding time for EN-Composite coatings.

3.4. Corrosion resistance measurements

Nyquist plots from the EIS measurements for the aluminium substrate, electroless Ni–P (annealed), Ni–P–WS_2 and Ni–P–WS_2 (annealed) composite coatings in 3.5%NaCl solution are given in figure 7. It is obvious that the obtained diagrams show a single semi circle and one capacitive loop. This behaviour is typical for solid metal electrodes that prove frequency dispersion of the impedance data and has been attributed to the roughness and other heterogeneities of the solid surface. An upgrading of the corrosion resistance of Ni–P–WS_2 (annealed) composite coatings compared to Ni–P (annealed) was also observed in this study.

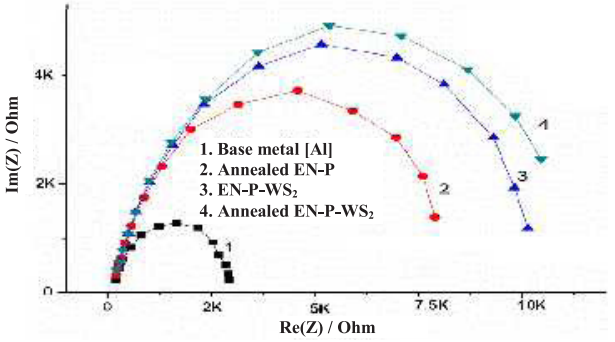

Fig. 7. Nyquist plots for electroless composite coatings.

Table 3. Evaluation of corrosion resistance of the coatings by impedance measurements: Electrolyte 3.5% NaCl

Deposit	R_t (Ohm cm^2)	C_{dl} (μF cm^{-2})
Aluminium	3200	15.2
Ni-P (Annealed)	8000	9.27
Ni-P-WS_2 (15 g l^{-1})	10643	5.53
Ni-P-WS_2 (Annealed)	12400	1.26

This could be due to the fact that the uniform distribution of WS_2 particles in Ni-P matrix is capable of filling some of the pores in the coating and impede further diffusion of chloride ions along the interface. It also can be observed that Ni–P– WS_2 with 15 $g.l^{-1}$ WS_2 in the bath formulation exhibits the biggest half circle radius compared to Ni-P coatings and aluminium substrate. The R_t and C_{dl} values of coatings are presented in Table 3. The R_t of Ni–P– WS_2 (annealed) with 15 $g.l^{-1}$ WS_2 and Ni–P (annealed) composite coating, are 12400 and 8000 $Ohm.cm^2$, respectively and the corresponding C_{dl} values are 1.26 and 9.27 $\mu F.cm^{-2}$, respectively. According to Li [16] and Karthikeyan et al [17] high values of R_t and low values of C_{dl} indicate better corrosion protective ability of coatings, while the

C_{dl} value is also related to the porosity of the coating. The composite coatings exhibited the best corrosion resistance, consistent with hardness and wear resistance results. Also, the enhanced corrosion resistance of WS_2coatings indicated that composite coatings are non-porous.

3.5. Effect of coating thickness

As the rate of deposition of electroless Ni-P-WS_2 composite coatings was found as 12 microns per hour, the deposition timings were increased to 6 hours to obtain coatings with thickness of 55 microns per hour by mechanical agitation. A suitable replenishment of nickel and hypophosphite was made by periodic analysis with optimized temperature and pH. Since the thickness of deposit was above 55 microns the developed coatings exhibited good mechanical properties.

3.6. Effect of particulate concentrations in the bath on the percentage of nickel and phosphorous in the deposit

Table 4 indicates that increasing concentrations of WS_2 in the bath enhance its incorporation into Ni-P matrix. In the present study, the increasing concentrations of WS_2 have lessened the percentage of nickel and phosphorus content in the deposits. An optimum concentration of 15 $g.l^{-1}$ of WS_2 is the recommended dosages for the bath. Beyond these, collisions among the moving particles inhibit the plating process.

Table 4. Effect of concentration of WS_2 particles in the bath on the percentage of Ni, P and WS_2 particle in the deposit

WS_2 in the bath g l^{-1}	**Composition of the deposit**		
	Nickel (%)	**Phosphorus(%)**	**WS_2 (%)**
0	89.18	10.82	--
5	87.69	9.79	2.52
10	84.79	9.28	5.93
15	84.68	9.04	6.28
25	86.26	8.66	5.08

The incorporation of WS_2 seems to be mechanical and little due to the electrophorectic effects of the hydrophobic particles. As the particles strike the surface they are included in the nickel alloy being deposited and become a part of the cermets. There is no molecular bond between WS_2 particles and the Ni-P matrix [18]. The composite is developed mechanically by the effect of settling and impinging of the WS_2 upon the substrate metal and subsequent envelopment of the particles by the matrix material, as they are codepositing. Evenly keeping WS_2 in suspension and rotating the object to be coated with in resonance by bath agitation can ensure uniformity of composition for the composites.

4. Conclusions

A novel Ni–P–WS_2 composite coating on aluminium metal has been developed by electroless plating process. X-ray diffractograms confirmed the crystalline state of coatings containing tungsten sulfide particles. The micro hardness, wear and corrosion resistance of Ni–P–WS_2 composite coatings have been significantly higher than Ni-P coatings. The low frictional coefficient of the coatings indicated that it can be used as solid lubricants to the sliding parts of aircraft machines.

5. References

[1] Singh, V.P., Sil, A. and Jayaganthan, Tribological behavior of nanostructured Al_2O_3 coatings, *Surface Engineering,* 2012, 8 (4), pp. 277-284.

[2] Karthikeyan, S., Srinivasan, K.N., Vasudevan, T. and John, S., Parametric studies on Electroless Ni-P-MoS_2 composite coatings, *Journal of Surface Engineering,* 2005, 2(1), pp. 72-75.

[3] Hu, X.G., Cai, W.J., Xu, Y.F., Wan, J.C. and Sun, X.J., Electroless Ni-P-(nano-MoS2) composite coatings and their corrosion properties**,** *Surface Engineering,* 2009, 25 (5), pp. 361-366.

[4] Zhao, Q. and Liu, Y., Electroless Ni-Cu-P-PTFE composite coatings and their anticorrosion properties, *Surface and Coatings Technology*, 2005, 200 (7), pp. 2510-2514.

[5] Srinivasan, K.N. and John, S., Composite coatings in Methane Sulphonic acid, *Surface Engineering*, 2005, 21 (2), pp. 156-160.

[6] Lim, S.C., Gupta, M., Goh, Y.S. and Seow, K.C., Wear resistant WC–Co composite hard coatings, *Surface Engineering,* 1997, 13(3), pp. 247-250.

[7] Karthikeyan, S., Karuppuchamy, S., Sakthivel, A.P., Vasudevan, T., Srinivasan, K.N. and John, S., *Journal of Surface Science and Technology*, 1999, 15 (3-4), pp. 116-124.

[8] Yu, T., Deng, Q.L., Zheng, J.F., Dong, G. and Yang, J.G., Microstructure and wear behaviour of laser clad NiCrBSi+Ta composite coating**,** *Surface Engineering*, 2012, 28 (5), pp. 357-363.

[9] Zarebidaki, A. and Allahkaram, S.R., Porosity measurement of electroless Ni-P coatings reinforced by CNT or SiC particles, *Surface Engineering*, 2012, 28 (6), pp. 400-405.

[10] Tulsi, S.S., Electroless Nickel-PTFE Composite Coatings, *Trans. Inst. Met. Finish*, 1983, 61 (4), pp. 142-149.

[11] Agarwal, A. and Dahotre, N.B., Mechanical characterisation of interface in laser surface engineered composite TiB2 coating on steel, *Surface Engineering*, 2001, 17(1), pp. 66-70.
[12] Karthikeyan, S., Venkatachalam, G., Srinivasan, K. N. and Narayanan, S., Development of Electroless Ni-P-BaSO4 composite coatings, *Journal of Electroplating & Finishing,* 2011, 30(06), pp. 16-19.
[13] Guo, Z., Zhu, X. and Xu, R., Microstructure and Wear Resistance of Electrodeposited RE–Ni–Mo–P–B4C–PTFE Composite Coatings, *Surface Engineering,* 2004, 20(2), pp. 113-116.
[14] Keong, K.G., Sha, W. and Malinov, S., Hardness evolution of electroless nickel-phosphorus deposits with thermal processing, *Surface and Coatings Technology*, 2003, 168, pp. 263-274.
[15] Sharma, S.B., Agarwala, R.C., Agarwala, V. and Ray, S., Application of Ni-P-ZrO 2-Al 2O 3-Al 3Zr electroless composite coatings and their characteristics, *Surface Engineering,* 2002, 18(5), pp. 344-349.
[16] Li, Q., Yang, Q.X., Zhang, L., Wang, J. and Chen, B., Corrosion resistance and mechanical properties of pulse electrodeposited Ni-TiO2 composite coating for sintered NdFeB magnet, *Journal of Alloys and Compounds*, 2009, 482, pp. 339–344.
[17] Karthikeyan, S., Srinivasan, K.N., Vasudevan, T., John, S., Gopalan, A. and Paruthimal Kalaignan, G., Electroless nickel – phosphorous – quartz composite coating, *Bulletin of electrochemistry*, 2001, 17, pp. 127-130.
[18] Hubbell, F.N., Chemically deposited composites - a new generation of electroless coatings, *Transactions of the Institute of Metal Finishing*, 1978, 56, pp. 65-69.